



Publication Year	2015
Acceptance in OA	2020-03-11T10:35:14Z
Title	Discovery of true, likely and possible symbiotic stars in the dwarf spheroidal NGC 205
Authors	Gonçalves, Denise R., MAGRINI, LAURA, de la Rosa, Ignacio G., Akras, Stavros
Publisher's version (DOI)	10.1093/mnras/stu2437
Handle	http://hdl.handle.net/20.500.12386/23199
Journal	MONTHLY NOTICES OF THE ROYAL ASTRONOMICAL SOCIETY
Volume	447

Discovery of true, likely and possible symbiotic stars in the dwarf spheroidal NGC 205^{*}

Denise R. Gonçalves,^{1†} Laura Magrini,² Ignacio G. de la Rosa^{3,4} and Stavros Akras¹

¹*Observatório do Valongo, Universidade Federal do Rio de Janeiro, Ladeira Pedro Antonio 43, 20080-090 Rio de Janeiro, Brazil*

²*INAF – Osservatorio Astrofisico di Arcetri, Largo E. Fermi 5, I-50125 Firenze, Italy*

³*Instituto de Astrofísica de Canarias, E-38205 La Laguna, Tenerife, Spain*

⁴*Departamento de Astrofísica, Universidad de La Laguna, E-38206 La Laguna, Tenerife, Spain*

Accepted 2014 November 16. Received 2014 November 16; in original form 2014 September 1

ABSTRACT

In this paper we discuss the photometric and spectroscopic observations of newly discovered (symbiotic) systems in the dwarf spheroidal galaxy NGC 205. The Gemini Multi-Object Spectrograph on–off band [O III] 5007 Å emission imaging highlighted several [O III] line emitters, for which optical spectra were then obtained. The detailed study of the spectra of three objects allows us to identify them as true, likely and possible symbiotic systems (SySts), the first ones discovered in this galaxy. SySt-1 is unambiguously classified as a symbiotic star, because of the presence of unique emission lines which belong *only* to symbiotic spectra, the well-known O VI Raman-scattered lines. SySt-2 is only possibly a SySt because the Ne VII Raman-scattered line at 4881 Å, recently identified in a well-studied Galactic symbiotic as another very conspicuous property of symbiotic, could as well be identified as N III or [Fe III]. Finally, SySt-3 is likely a symbiotic binary because in the red part of the spectrum it shows the continuum of a late giant, and forbidden lines of moderate to high ionization, like [Fe V] 4180 Å. The main source for scepticism on the symbiotic nature of the latter systems is their location in the planetary nebula region in the [O III]4363/H γ versus [O III]5007/H β diagnostic diagram. It is worth mentioning that at least another two confirmed symbiotics, one of the Local Group dwarf spheroidal IC 10 and the other of the Galaxy, are also misplaced in this diagram.

Key words: binaries: symbiotic – galaxies: dwarf – galaxies: individual: NGC 205 – Local Group.

1 INTRODUCTION

Symbiotic stars (SySts) are binary systems composed by a cool giant star and a hot companion, which can be a white dwarf, a main-sequence star with accretion disc or a neutron star. The wind expelled by the cool giant star accretes onto the hot companion powering the symbiotic activity, including occasional eruptions and jets.

Symbiotic systems display characteristic spectra, which allow their detection with on–off band techniques, in which narrow-band filters are tuned in to one or more typical emission lines. In an attempt to separate symbiotic systems from their most common mimic, Magrini, Corradi & Munari (2003) used several diagnostic

diagrams based on the fluxes obtained with the narrow-band filters H α and [O III] at 5007 Å. They concluded that it is, indeed, possible to discover symbiotic systems using their proposed diagrams, but it is not easy to discriminate them from planetary nebulae (PNe) or compact H II regions without a spectroscopic follow-up. They also estimated the expected number of SySts in a given galaxy, finding that it increases with the luminosity (mass) of the galaxy. For a galaxy like NGC 205, the second most massive dwarf companion of Andromeda ($3.3 \times 10^8 M_{\odot}$; McConnachie 2012), the predicted number of SySts is 1.7×10^4 (Magrini et al. 2003), including both active and inactive systems. Active systems are spectroscopically detectable because their stars are interacting and exchanging matter.

This figure is an absolute estimation, and, obviously, it has to be rescaled to obtain the number of SySts that can actually be observed. If the ratio of known (up to 300; Miszalski & Mikolajewska 2014; Rodríguez-Flores et al. 2014) versus expected (400 000; Magrini et al. 2003) SySts in our Galaxy is assumed to be valid in NGC 205, around ~ 12 SySts are expected to be active and detectable in NGC 205. In general, SySts are expected to be more abundant in dwarf

^{*}Based on observations obtained at the Gemini Observatory, which is operated by the Association of Universities for Research in Astronomy, Inc., under a cooperative agreement with the NSF on behalf of the Gemini partnership.

[†]E-mail: denise@astro.ufrj.br

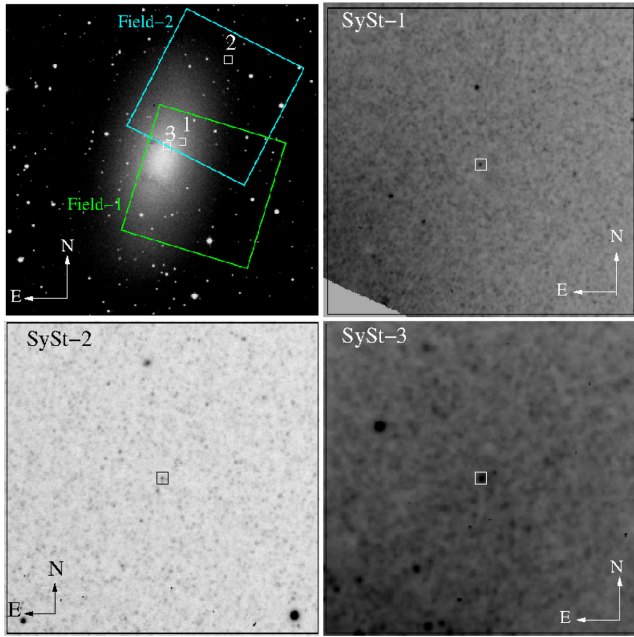


Figure 1. Top right: a 14.2×14.2 arcmin² POSSII image of NGC 205, retrieved from the NASA/IPAC Extragalactic Database. The two FoV (5.5×5.5 arcmin²), observed with GMOS@Gemini, are superimposed on the POSSII image. The position of the three symbiotic systems are also highlighted with small boxes within 1.0×1.0 arcmin² finding charts of the newly discovered systems: top right – centred on SySt-1; bottom left – centred on SySt-2; bottom right – centred on SySt-3.

spheroidal (dSph) than in dwarf irregular (dIrr) galaxies (Magrini et al. 2003).

In this work, the discovery of the first three (true, likely and possible) SySts of NGC 205 is reported as a result of our spectroscopic study of the emission-line population of the galaxy. This paper is organized as follows: in Section 2 we describe our observations, while in Section 3 we present the spectroscopic characterization of the three systems. In Section 4 we give an estimate of the stellar parameters of the hot and cool companions in the objects. The location of the newly discovered systems in the Gutierrez-Moreno, Moreno & Cortés (1995) diagnostic diagram, aimed to separate SySts from PNe, is discussed in Section 5. We summarize our work and give our conclusions in Section 6.

2 OBSERVATIONAL DATA

We obtained the present data by using the imager and spectrograph, Gemini Multi-Object Spectrograph (GMOS), at the GEMINI North telescope, in 2010 (Programme GN-2010B-Q-107). The GMOS has a 5.5×5.5 arcmin² field of view (FoV), which was centred at the RA/DEC 00:40:12.50/+41:40:03 (Field-1; F1) and 00:40:10.50/+41:43:47.0 (Field-2; F2) of NGC 205, as indicated in Fig. 1.

We adopted the on–off band imaging technique to identify strong emission-line objects (mainly PNe) with the on-band filter [O III], O III_G0318, and the off-band one, [O III]-Continuum, being O III_G0319. The central wavelength and width of these two filters are 499 nm/5 nm, and 514 nm/10 nm, respectively. Three exposures of 540 (810) s using the on-band (off-band) filter were taken, in July 9 (F1) and September 2 and 3 (F2) of 2010. We then used the two combined narrow-band frames to build an [O III] continuum-

Table 1. Coordinates of the three SySts. F1 (F2) stands for Field-1 (Field-2) GMOS@Gemini FoV we observed. See Fig. 1.

Field-ID	Name	RA J2000.0	Dec J2000.0	C05 ^a
F2-9	NGC 205 SySt-1	00:40:17.60	+41:41:53.30	–
F2-8	NGC 205 SySt-2	00:40:07.97	+41:45:23.64	PN18
F1-18	NGC 205 SySt-3	00:40:20.97	+41:41:42.60	PN36

^aPN ID used by Corradi et al. (2005, C05).

subtracted image of the field, from which we identified a number of objects to be spectroscopically observed, including previously known PNe and other [O III] emission-line objects. In Table 1 we also give the Field-ID of the symbiotics, for the sake of consistence with the results for the PNe, which were discussed in a previous paper (Gonçalves et al. 2014, hereafter G14).

The spectroscopy of F1 and F2 was obtained with two gratings, R400+G5305 and B600, from 2010 October 8–11. The effective spectral coverage of the spectra is $3600\text{--}9400 \pm 400$ Å, with initial and final λ depending on the location of the slit. Exposure times were of 3×2400 s per grating. The disperser central wavelength was slightly varied from exposure to exposure (750 ± 10 nm for R400+G5305, and B600 was centred at 460 ± 10 nm). The slit width was 1 arcsec, while the slit height was 5.6 arcsec. The final (binned) spatial scale and reciprocal dispersions of the spectra are as follows: 0.161 arcsec and 0.09 nm per pixel, with B600; and 0.161 arcsec and 0.134 nm per pixel, with R400+G5305. The seeing varied from ~ 0.42 to ~ 0.57 arcsec. CuAr lamp exposures were obtained with both gratings, in the day before or after the science exposures, for wavelength calibration. On 2010 October 8 and 12, we obtained spectra of spectrophotometric standards (Massey et al. 1988; Massey & Gronwall 1990) with the same instrumental setups as for science exposures and we used them to flux calibrate the spectra. The whole reduction and calibration was performed in the standard way by using the Gemini GMOS data reduction script and LONG-SLIT tasks, both being part of IRAF. We refer the reader to G14 for further details on the observations and reduction where we described, among others details, the effects of the differential atmospheric refraction on the present data. In G14 we also show the good agreement between our measured spectroscopic fluxes and those extracted from the literature for common objects.

2.1 Spectroscopic measurements and analysis

The emission-line fluxes were measured with the IRAF package SPLIT. Errors on the fluxes were calculated taking into account the statistical errors in the measurement of the fluxes, as well as systematic errors (flux calibrations, background determination and sky subtraction). The resulting errors are given in the fluxes table (Table 2). The Balmer Decrement was used as an estimation of the internal dust attenuation of the SySts. Given that H δ and H γ were measured at a relatively noisier part of the spectrum, they are not useful for deriving the extinction correction constant, c_β . Thus, c_β was determined comparing the observed Balmer $I(H\alpha)/I(H\beta)$ ratio with its theoretical value, 2.85 (Osterbrock & Ferland 2006). The $c_\beta = 0.445 \pm 0.04$ obtained with the Balmer Decrement, for NGC 205 SySt-1, compares nicely with the mean c_β we found in G14 for the PNe of NGC 205, 0.38 ± 0.09 . The c_β for the other two systems, on the other hand, are very low: 0.168 ± 0.078 and 0.00 ± 0.54 for NGC 205 SySt-2 and 3, respectively. Though low, such values are not uncommon within those of the nebular systems either in F1 or in F2 of G14 (see their table A1).

Table 2. Observed fluxes (F_λ) and extinction corrected intensities (I_λ) of NGC 205 SySt-1, 2 and 3. The observed H β flux is in units of 10^{-16} erg cm $^{-2}$ s $^{-1}$, and both I_λ and F_λ are normalized to H β = 100. Errors, obtained for different flux ranges, are up to 6, 15, 25, 40 and >50 per cent for $F_\lambda > 100$, 10–100, 1–10, 0.1–1.0 and 0.01–0.1 $F_{H\beta}$, respectively. ‘:’ indicate very uncertain measurements, due to loosely defined continuum.

$F_{H\beta}$	c_β	Ion	λ (Å)	I_λ	F_λ
<i>NGC 205 SySt-1</i>					
3.700	0.445 ± 0.04	[Ne III]	3868	16.60	12.30
		[Ne III]+He I	3968	22.20	16.87
		N III	4003	19.66	15.08
		–	4084	10.27	8.064
		H δ	4100	36.41	28.73
		H γ	4340	72.00	61.22
		[O III]	4363	42.92	36.77
		He I	4437	9.926	8.706
		C II+O II	4491	8.156	7.280
		Fe II	4584	5.230	4.810
		O II	4638	5.040	4.713
		He II	4686	124.2	117.8
		H β	4861	100.0	100.0
		[O III]	4959	34.19	35.06
		[O III]	5007	102.2	106.1
		He I	5016	4.032	4.200
		[Fe VII]	5159	7.891	8.500
		[Fe II]	5261	3.112	3.429
		Fe III	5275	3.756	4.151
		[Ca V]	5308	3.113	3.493
		[Fe II]	5376	1.384	1.562
		He II	5412	4.917	5.587
		[Fe II]	5496	2.219	2.562
		[Fe II]	5582	21.25	24.93
		V II	5618	4.195	4.950
		[Fe VII]	5720	10.19	12.23
		[N II]	5755	2.189	2.648
		He I	5876	11.12	13.70
		[Ca V]+[Fe II]	6086	12.84	16.29
		[O I]	6300	3.534	4.621
		[S III]	6312	1.414	1.853
		H α	6563	307.2	416.4
		[N II]	6584	2.774	3.770
		He I	6678	2.253	3.101 :
		[S II]	6717	0.508	0.703 :
		[S II]	6731	0.865	1.199 :
		[Fe VI]	6739	0.610	0.847 :
		O VI Raman	6830	28.41	39.93 :
		He I	7065	2.841	4.123 :
		O VI Raman	7088	5.426	7.899 :
		[O II]	7320	0.890	1.338 :
		[O II]	7330	0.982	1.478 :
		[O I]	8447	3.776	6.550 :
<i>NGC 205 SySt-2</i>					
0.740	0.168 ± 0.078	H γ	4340	80.42	75.69
		[O III]	4363	52.24	49.31
		He II	4686	137.4	134.8
		H β	4861	100.0	100.0
		Ne VII Raman ?, N III ?, [Fe III] ?	4881	30.11	30.16
		N III?	4898	13.37	13.42
		[O III]	4959	233.5	235.8
		[O III]	5007	694.3	704.5
		He I	5876	12.44	13.45
		H α	6563	293.9	329.7 :

Table 2 – *continued*

$F_{H\beta}$	c_β	Ion	λ (Å)	I_λ	F_λ
		–	6783	34.00	38.58 :
		–	7167	11.06	12.80 :
		–	8107	19.82	24.05 :
		–	8782	40.42	50.41 :
		[S III]	9069	24.79	31.19 :
<i>NGC 205 SySt-3</i>					
1.263	0.00 ± 0.54	[O II]	3729	21.6	21.6
		[Ne III]	3868	32.7	32.7
		H δ	4100	25.3	25.3
		[Fe V]	4180	35.3	35.3
		H γ	4340	54.8	54.8
		[O III]	4363	16.4	16.4
		–	4553	82.89	82.89
		He II	4686	84.8	84.8
		H β	4861	100.0	100.0
		[O III]	4959	295.4	295.4
		[O III]	5007	860.1	860.1
		–	5343	22.1	22.1
		[Fe II]	5582	220.5	220.5
		–	5586	76.0	76.0
		H α	6563	179.2	179.2 :

The H β flux ($F_{H\beta}$), the extinction correction constant (c_β), all the extinction corrected line intensities (I_λ) as well as emission-line fluxes (F_λ), are shown in Table 2.

3 THE SYSTEMS’ DISCOVERY

The three emission-line objects were serendipitously discovered in the spectroscopic study of NGC 205. Their spectra revealed features that are characteristic of symbiotic systems (see e.g. Belczyński et al. 2000). In the optical, the spectra of symbiotics are indeed notable due to the absorption features and continuum of late-type M giants, strong nebular emission lines of Balmer H I, the recombination lines of He I and He II and the forbidden lines of [O II], [Ne III], [Ne V] and [Fe VII]. In more detail, the well-known criteria to identify SySts (Belczyński et al. 2000) are the following: (i) the presence of the absorption features of a late-type giant (like titanium and vanadium oxides, TiO and VO, H $_2$ O, CO and CN bands, as well as Ca I, Ca II, Fe I and Na I absorption lines). (ii) The presence of strong H I and He I emission lines and either emission lines of ions with an ionization potential of at least 35 eV (e.g. [O III]), or an A- or F-type continuum with additional shell absorption lines from H I, He I and singly-ionized metals. The latter corresponds to the appearance of a symbiotic star in outburst. (iii) The presence of the λ 6830 Å emission line, even if no feature of the cool star is found. Also, very recently, Lee et al. (2014) identified another Raman-scattered Ne VII λ 973 at 4881 Å line, in the spectrum of the Galactic symbiotic star V1016 Cygni. The latter scattering process is again a characteristic of symbiotic systems.

The three systems in NGC 205, hereafter NGC 205 SySt-1, NGC 205 SySt-2, NGC 205 SySt-3, show the following characteristics that led us to classify them, respectively, as true, possible and likely symbiotic binaries.

(1) NGC 205 SySt-1 shows the O VI Raman-scattered lines at 6830 Å, 7088 Å, unique signatures seen only in SySts (Schmid 1989). These emission lines provide a firm classification criterion of symbiotic systems, even when the red giant continuum is not directly observed, as discussed above. Moreover, in the present

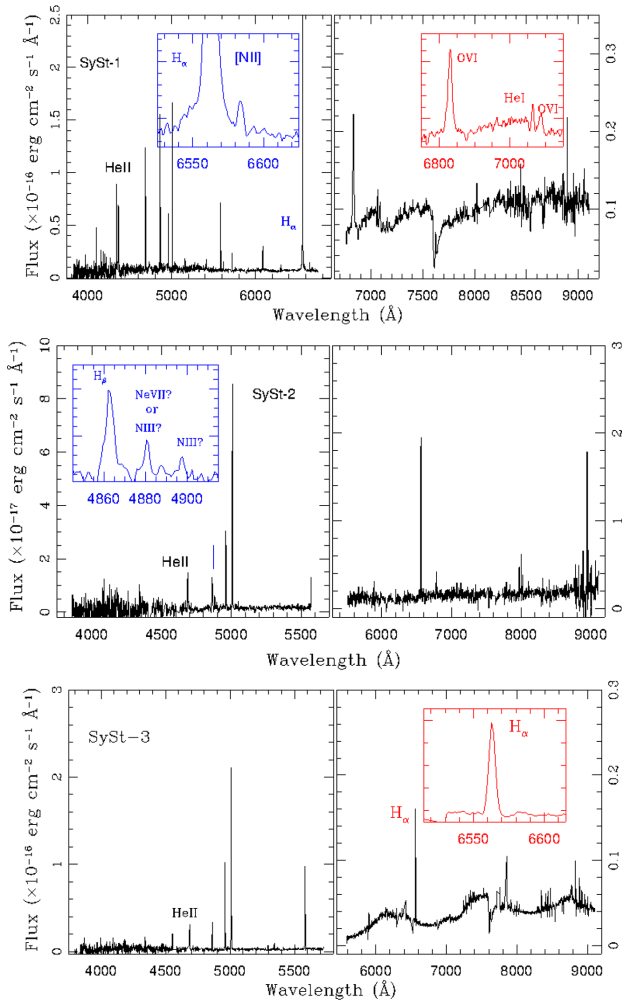


Figure 2. GMOS blue plus red spectra of NGC 205 symbiotic systems. SySt-1: the inset at the blue part of the spectrum shows the typical single-peaked broad $H\alpha$ profile, with a shoulder at the blue side, similar to well-known Galactic symbiotics (Tomova & Tomov 1999; Leedj arv et al. 2004). The red side inset highlights the $O\text{VI}$ Raman-scattered lines (at 6830 and 7088 Å), which are also broad if compared to the forbidden lines present in the spectrum (Schmid et al. 1999). Note the intense red continuum of the companion star that makes the fluxes measured in this part of the spectrum very uncertain. SySt-2: the inset shows the $H\beta$ as well as the Raman-scattered $\text{Ne VII } \lambda 973$ (see Lee, Heo & Lee 2014) or N III at 4881 Å line. A third possibility for this line feature is $[\text{Fe III}]$. Another, not well-identified, line also shows up as a relatively intense line at 4898 Å. If the feature at 4881 Å is confirmed as N III emission line, so the one at 4898 Å would also be identified as another N III line (see Table 2). SySt-3: as in SySt-2, $\text{He II } \lambda 4686$ line is very intense. The inset shows the $H\alpha$ line, the only one we measured in the red part of the spectrum. The cool star continuum is very prominent, again making the emission-line flux measurements very uncertain. Another conspicuous feature, in all the three blue spectra above, is the $\text{He II } \lambda 4686$ line, whose intense fluxes (see Table 2) imply $T_{\text{eff}} > 270\,000$ K in the three cases. Also note that CCD gaps were masked in all the spectra (see Section 2). The resulting spectral discontinuities can be seen, for instance, around 7950, 8050 and 8150 Å in the upper-right panel.

case the absorption features of the M giant component are clearly seen. The discovery of NGC 205 SySt-1 is similar to that of other SySts in the Local Group (LG) galaxies, as in the case of NGC 6822 (Kniazev et al. 2009) and NGC 185 (Gonçalves et al. 2012), in which the $O\text{VI}$ Raman-scattered lines were also detected.

(2) NGC 205 SySt-2, on the other hand, has an extremely intense $\text{He II } \lambda 4686$ Å emission line, property that is included among the classification criteria of SySts (Fig. 2, middle panel). As a consequence of such an intense doubly ionized He emission, the effective temperature (T_{eff}) of the star that ionizes the gas should be tremendously high (see Section 4.1). In spite of a high T_{eff} , it is puzzling the fact that higher ionization forbidden lines are not detected in its spectrum, unlike in SySt-1. A possible reason would be the fact that the present system is significantly fainter than the latter (Table 2 shows $H\beta$ fluxes of 3.70 and 0.74×10^{-16} erg $\text{cm}^{-2} \text{s}^{-1}$ for SySt-1 and 2, respectively). In addition, and as far as we know for the first time in an extragalactic SySt, we tentatively identified the $\text{Ne VII } \lambda 973$ at 4881 Å Raman-scattered line in the spectrum of SySt-2. This feature can be clearly seen in the inset of the middle panel of Fig. 2 (and in Table 2). However, also considering the fact that in the present case only Ne VII is present, with no sign of the $O\text{VI}$ Raman-scattered line (both were found at the same epoch in V1016; Lee et al. 2014), the emission line at 4881 Å could as well be a N III line. In this case the line at $\lambda 4898$ Å, also present in the spectrum and for which we could not easily find an identification, might be associated with N III too. Considering the low-resolution of the present spectrum, the other lines from the N III multiplet are blended with $H\beta$, further complicating a strong identification as N III . And, a third possible identification for the 4881 Å emission-line would be $[\text{Fe III}]$. Altogether, the latter arguments imply that the other possible identifications (N III and $[\text{Fe III}]$) are at least equally possible as $\text{Ne VII } \lambda 973$ at 4881 Å Raman-scattered line.

(3) NGC 205 SySt-3 was discovered because of the clear presence of a cool stellar continuum in the red part of its spectrum, compatible with that of an M giant. This symbiotic star, as well as the one discovered in the LG dIrr galaxy IC10 (Gonçalves et al. 2008), though not showing the Raman-scattered lines, shares some other properties of Galactic sources. The latter includes the moderate to high-ionization $[\text{Fe V}]$ line, at 4181 Å (see, for instance, Gutierrez-Moreno & Moreno 1996). These two conspicuous properties of SySts lead us to conclude that SySt-3 is, likely, a symbiotic system.

We compare our detections with other literature surveys in NGC 205 also interested in emission-line populations, in particular PNe: Ford et al. (1973), Ciardullo et al. (1989), Richer & McCall (1995, 2008), Corradi et al. (2005) and Merrett et al. (2006). All these surveys studied this galaxy using narrow-band imaging and/or optical spectroscopy. From these works, only the spectroscopic survey of Richer & McCall (1995 and 2008) could have found out our symbiotics. However, targets in Table 1 are not included among theirs. The NGC 205 SySt-1 is also not listed among the objects analysed – via narrow-band imaging – by Corradi et al. (2005), while they detected the other two systems and the correspondent ID in their survey are also given in Table 1. The most probable reason why SySt-1 was not detected by Corradi et al. (2005) is that the completeness limit of their survey was only 50 per cent in $\text{mag}([\text{O III}]) = 24.5$ – where $\text{mag}([\text{O III}]) = -2.5 \log F([\text{O III}]5007) - 13.74$ (Ciardullo et al. 1989). $[\text{O III}]$ magnitudes of 24.8, 24.4 and 23.6 are the present magnitudes of SySt-1, 2 and 3, respectively.

In Fig. 1 we show the fields we observed with GMOS, and the finding charts of the three newly discovered SySts. Their coordinates, as well as their IDs in G14 and Corradi et al. (2005) are given in Table 1. Compositions of the blue plus red portions of the GMOS spectra of NGC 205 symbiotics are shown in Fig. 2, where the main properties that make of them symbiotic systems are highlighted.

4 CHARACTERIZATION OF THE SYMBIOTIC SYSTEMS

4.1 The ionized nebulae and the ionizing sources

We have determined the above discussed extinction coefficient, and corrected all the measured fluxes for further analysis, despite the fact that the Balmer line ratios in many symbiotic nebulae indicate self-absorption effects (due to high densities). In those circumstances, the standard methods to estimate reddening would not apply (possibly the case in SySt-2 and 3). Though most of the line ratios that would provide electron temperatures and densities comes to be out of the sensitive range (see Osterbrock & Ferland 2006), the sulphur doublet [S II] $\lambda\lambda 6716, 6731$ allowed us to estimate an electron density of 6000 cm^{-3} for SySt-1 (since the [O III]-temperature sensitive ratio is below the lower limit, for the above calculation we adopted $T_e = 21\,000 \text{ K}$). The density sensitive lines were not measured in the remaining cases. [O III] electron temperatures can be derived from the [O III] $\lambda\lambda 4959, 5007$ doublet to the $\lambda 4363$ line ratio. Relatively high T_e [O III] of $>21\,000$ and $14\,500 \text{ K}$ were found for SySt-2 and 3, respectively. Also, using the extinction-corrected integrated flux of He II $\lambda 4686$ (Kaler & Jacoby 1989), we derived T_{eff} of $>340\,000$, $>340\,000$ and $270\,000 \text{ K}$ as the temperature of the hot companion, which represents the main nebular ionizing source, of SySt-1, 2 and 3, respectively.

The diagnostics derived above constitute further evidences in favour of our targets being representative of symbiotic systems, since T_e and T_{eff} are much higher than the typical values for these parameters found either in PNe or compact H II regions.

4.2 The spectral classification of the cool companions

Having only the optical spectrum of the system it is hard to obtain the properties of the cool companion. However, limits to the spectral types based on the red part of the optical spectrum of SySts are possible (Kenyon & Fernández-Castro 1987). These authors, using their own data as well as the literature, pointed out that:

- (i) there is no evidence for measurable TiO absorption in stars earlier than the spectral type K4;
- (ii) TiO indices increase monotonically with spectral type from K4 to M6;
- (iii) VO bands, like the one at 7865 \AA , appear only in giants cooler than M5;
- (iv) the amount of VO absorption is negligible for stars earlier than M4, but rises rapidly for M4–M7.

Taking all these limits into account, and the spectra we show in Fig. 3 (on which neither the 7865 \AA , nor any other VO features are present), it is clear that the stars there represented have spectral types from K4 to M4. In order to avoid the tricky task of defining a common continuum, below which the TiO absorption indices could be measured (Kenyon & Fernández-Castro 1987), we refer the reader to Kirkpatrick et al. (1991), who provide an extensive spectral catalogue for late-type stars from classes K5 to M9, covering the wavelengths from 6900 to 9000 \AA . This region encompasses TiO and VO bands – key bands to classify early- and late-M stars. Table 5 and fig. 5 of their paper give the features found in late-K to late-M red spectra, and provide us with a more accurate range of spectral classes for the cool stars of NGC 205 SySt-1 and SySt-3, as being K5–M2 red giant (see Kirkpatrick’s fig. 5a and b against our Fig. 3). To perform this classification, our GMOS spectra had their spectral resolution smoothed to 18 \AA per pixel, in order to better compare

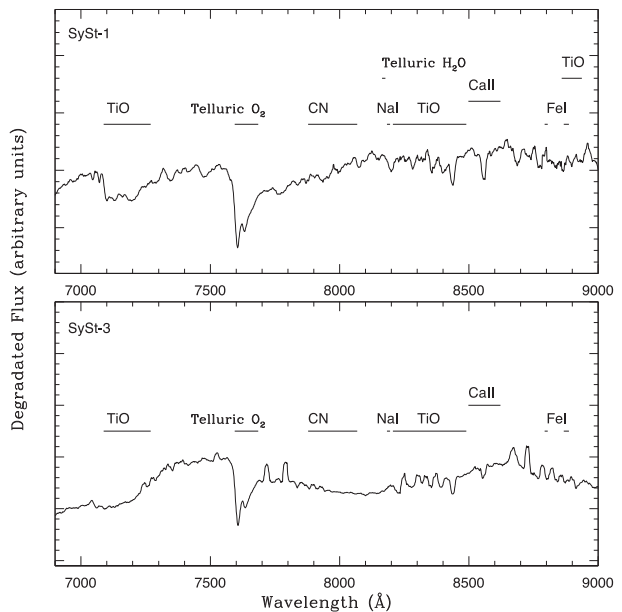


Figure 3. The 6900–9000 \AA range of the red spectrum of NGC 205 SySt-1 and 3, smoothed to match the spectral resolution of the Kirkpatrick, Henry & McCarthy (1991) catalogue ($18 \text{ \AA pixel}^{-1}$). Following Kirkpatrick et al. (1991), the most prominent features, key to determine the spectral type, are identified. (i) The CN bands are obvious in supergiants, weaker in giants and not seen in dwarfs. (ii) The TiO whose head band is at 8206 \AA is very strong in mid-M. (iii) The Ca II bands are strong from late-K to mid-M, strongest in supergiants and very weak in dwarfs. (iv) Fe I absorptions (at $8793\text{--}8805 \text{ \AA}$) are found in giants as well as supergiants.

to Kirkpatrick et al. (1991) catalogue. To close this analysis, we remember that the T_{eff} of K and M stars ranges, roughly, from 3700 to 5200 K and from 2400 to 3700 K, respectively.

4.3 The SED for SySt-1

Due to the extragalactic location of the stars, resolved photometric information is only available from selected telescope–instrument combinations, producing small point spread functions (PSFs) over pixels of an appropriate scale. Neither optical nor IR counterparts had been found for SySt-2 and SySt-3, probably because they are significantly much fainter than SySt-1 (the $F_{\text{H}\beta}$ of these two sources are ~ 7 and ~ 3 times lower than in SySt-1).

The spectral energy distribution (SED) of SySt-1, in Fig. 4, has been constructed with available information from the optical and IR spectral ranges. In addition to our optical [O III] image of SySt-1, presented in Section 2, the object has been unambiguously detected by *Hubble Space Telescope*-Wide Field Planetary Camera 2 (*HST*-WFPC2) and *Spitzer*-Infrared Array Camera (*Spitzer*-IRAC). All images have been retrieved from public archives, those from the *HST* come from the Mikulski Archive for Space Telescopes (MAST), while those from *Spitzer*-IRAC have been obtained from the NASA/IPAC Infrared Science Archive (IRSA). The *HST*-WFPC2 images, with detections in four filters ($F255W$, $F336W$, $F555W$ and $F675W$) have a $0.0996 \text{ arcsec pixel}^{-1}$ scale, with a PSF of typically 2 pixels full width at half-maximum (FWHM). Aperture photometry was carried out by ourselves using the IRAF package APPHOT and converted into flux density. The IR images from *Spitzer*-IRAC provide object detections in the four IRAC wavelengths (3.6, 4.5, 5.8 and $8 \mu\text{m}$). The *Spitzer*-IRAC pixel size is $1.2 \text{ arcsec pixel}^{-1}$ and the typical FWHM of the IRAC-1 PSF is 2.7 pixels. The IR

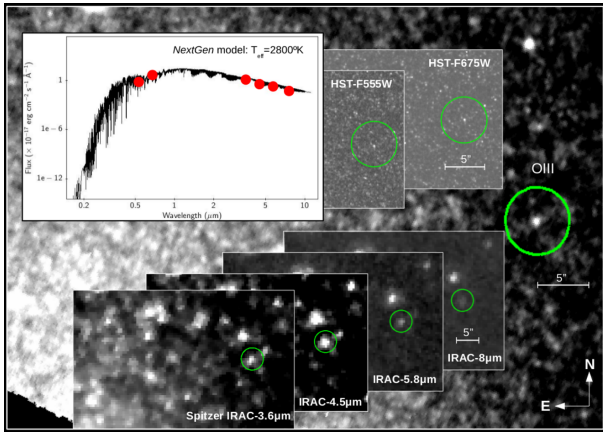


Figure 4. SED-fitting and multiwavelength observations, from *HST* and *Spitzer*-IRAC, are superimposed over the $[O\text{ III}]\lambda 5007$ image of SySt-1. SED points are photometrically extracted from the observations and the error bars are smaller than the dot size. The best SED-fitting, carried out with VOSpec tool, shows a NextGen Model (Hauschildt et al. 1999) with $T = 2800$ K.

photometric values for the flux density are taken directly from the *Spitzer*-IRAC pipeline. We have carefully checked that the lack of detection of the SySt-1 in several popular surveys as, SDSS, 2MASS, *WISE* is simply due to insufficient spatial resolution.

The final SED has been constructed with six points from both the *HST*-WFPC2 (2) and *Spitzer*-IRAC (4). The SED points corresponding to filters *HST*-F255W and F336W have been excluded. Although visually discernible, their photometric signal to noise is too low (~ 2). Flux values have been corrected for Galactic extinction, which according to Schlafly & Finkbeiner (2011) amounts to $A_V = 0.170$ mag. In addition to Galactic extinction, internal dust attenuation in the SySt-1 has an extinction constant $c_\beta = 0.45$ (see Section 2.1), calculated via the Balmer Decrement. Assuming an $R_V = 3.1$ extinction law, we deduce an $A_V = 0.955$ mag, also used to correct the observed SED values for reddening.

Model fitting has been carried out with the VOSpec tool from the European Space Agency-Virtual Observatory Project (ESA-VO Project). In addition to the crude blackbody fitting, which gives $T_{\text{eff}} = 2455$ K, we have fitted cool-star NextGen Models (Hauschildt et al. 1999), which produce best fitting for $T_{\text{eff}} = 2800$ K. We must emphasize that – though the agreement of the latter effective temperatures with the M red giant classification we obtained in Section 3.2 is very good – fittings are just indicative, because the *HST* optical SED points are probably overestimations of the continuum, as they include intense emission lines in their passbands, $[O\text{ III}]\lambda 5007$ in the F555W and $H\alpha$ in the F675W.

5 DIAGNOSTIC DIAGRAM: SEPARATING SySts FROM PNe

Gutierrez-Moreno et al. (1995) demonstrated that SySt can be separated from PNe in $[O\text{ III}]\lambda 4363/H\gamma$ versus $[O\text{ III}]\lambda 5007/H\beta$ diagram, being this separation mainly due to difference in physical conditions of the two kind of objects, especially the significantly lower density in PNe. The same is true for all the 35 recently discovered SySts in M31 (see fig. 5 in Mikolajewska, Caldwell & Shara 2014).

In Fig. 5 we place in the Gutierrez-Moreno et al. (1995) diagram all the SySt of the LG dwarf galaxies, for which the emission-line ratios are available. Most of them are indeed located in the loci of the SySts as studied by Gutierrez-Moreno et al. (1995) in the Galaxy, and by Mikolajewska et al. (2014) in M31. From this figure

it is clear that our SySt-1 is a true symbiotic system, and, at a first glance, the other two objects would be discarded as such.

However it is important to note that another symbiotic discovered in IC10, an LG dwarf galaxy (Gonçalves et al. 2008), is also misplaced in this diagram. In the case of the IC10 SySt-1, alike SySt-2 and 3 of NGC 205, neither highly ionized emission-lines nor Raman-scattered lines are found in the spectrum. The basis for the classification of the IC10 SySt-1 was the extreme similarity of its red spectrum with that of a well-known Galactic symbiotic, Hen 2-147 (Munari & Zwitter 2002), on which the cool companion features are clearly present. We also searched in the literature the emission-line ratios of Hen 2-147 to properly place it in the Gutierrez-Moreno et al. (1995) diagnostic diagram. The result, based on Mikolajewska, Acker & Stenholm (1997) ($[O\text{ III}]/H\gamma = 1.8$ and $[O\text{ III}]/H\beta = 12.5$), again moves this Galactic SySt in the loci of PNe, more exactly in the regime of young PNe. Because of their high densities, young PNe and SySts occupy the same region in this diagram, as pointed out by Gutierrez-Moreno et al. (1995) and Pereira & Miranda (2005). Therefore, what we show in Fig. 5 is that our SySt-2 as well as the known Galactic SySt Hen 2-147 occupy the young PN region of the diagram, whereas our SySt-3 and the known SySt-1 of IC10 are placed in the region of the evolved PNe. Altogether this seems to indicate that not only two of the (possible and likely) SySts in NGC 205, but also other known SySts are misplaced in this diagram, probably due to other effects than the density. Gutierrez-Moreno et al. (1995) also pointed out the fact that very young PNe and D-type SySts are sometimes impossible to be separated in their diagram.

Noting that the Milky Way has similar metallicity as M31 (Mikolajewska et al. 2014), and that most of the SySts of these two spiral galaxies are placed in similar regions of the Gutierrez-Moreno et al. (1995) diagnostic diagram, we also investigate the possible metallicity effects in the diagram. We did so by placing on it the SySts of the lower-metallicity LG dwarf galaxies. Fig. 5 shows that, even at the lower metallicities of the LG dwarf galaxies, this effect is insufficient to significantly change the loci of PNe and SySts in the diagram.

Finally, it is worth mentioning the fact that, at variance with most of the SySt candidates that were identified as so via $H\alpha$ narrow-band imaging – and then their spectra were taken to confirm the

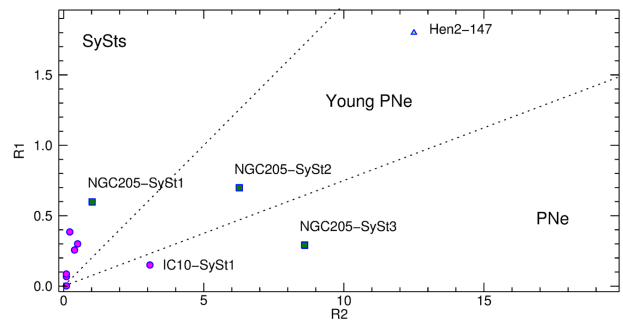


Figure 5. The diagnostic diagram to separate SySts from PNe: $R1 = [O\text{ III}]\lambda 4363/H\gamma$ versus $R2 = [O\text{ III}]\lambda 5007/H\beta$; as proposed by Gutierrez-Moreno et al. (1995). Boxes represent the objects discussed in this paper, whose line ratios are presented in Table 2. The circles represent seven symbiotic systems found in LG dwarf galaxies, for which the line ratios were published (LMC1, Morgan 1992; LMC-Sanduleak and LMC-S63, Allen 1980); or for which limits can be obtained from the published spectra (IC10, Gonçalves et al. 2008; NGC 185, Gonçalves et al. 2012; NGC 6822, Kniazev et al. 2009). The triangle represents the Galactic SySt Hen 2-147 whose line ratios were published by Mikolajewska et al. (1997).

classification of the objects – in this paper the narrow-band images were centred on the [O III] 5007 filter. This is probably why our SySts are much brighter in [O III] than the majority of the known SySts.

6 SUMMARY

In this paper, we report the discovery of the first three true, likely and possible SySts of the dSph galaxy NGC 205. Photometric and spectroscopic data of these objects were obtained with the GMOS, installed on the Gemini North 8.1-m telescope. Among the detection of several [O III] line emitters in the NGC 205, three objects were identified as SySts.

The classification of these sources as SySts was done based on the identification of the Raman scattering O VI lines around $\lambda\lambda 6830, 7088 \text{ \AA}$ and Ne VII of 4881 \AA (SySt-1 and SySt-2), the direct observation of the red continuum of the cool companion (SySt-1 and SySt-3), the extremely high intensity of the He II 4846 \AA recombination line (SySt-1, SySt-2 and SySt-3) and the presence of moderate to high-ionization forbidden lines (for instance [Fe V] and [Fe VII]), in SySt-1 and -3. If confirmed as a true symbiotic binary, SySt-2 will be the second known symbiotic star (and the first extragalactic one) that shows the Ne VII Raman scattering line at 4881 \AA .

The effective temperature of the hot companions were estimated $>340\,000 \text{ K}$ for SySt-1 and SySt-2 and $\sim 270\,000 \text{ K}$ for SySt-3. These extremely high temperatures are consistent with the detection of high-excitation emission lines in the spectra of SySt-1 and -3 (e.g. O VI, [Fe VII], Ne VII). Being the faintest of the three systems here studied, SySt-2 is an exception in having [O III] as its highest ionization forbidden line.

By examining the red continuum spectra of the cool companions, they were classified as K5–M2 red giants. It is worth mentioning that the classification of the cool companion in SySt-1 as an M2 III is consistent with a cool-star NextGen stellar atmospheric model of $T_{\text{eff}} = 2800 \text{ K}$. This kind of analysis as well as the classification of the cool companion is, unfortunately, not feasible for SySt-3.

We discuss the location of the newly discovered systems in the Gutierrez-Moreno et al. (1995) diagram, meant to separate SySts from PNe in [O III]4363/H γ versus [O III]5007/H β plane. From their location in this diagnostic diagram, only SySt-1 would be a true symbiotic system. Our SySt-2 as well as the known Galactic SySt Hen 2-147 occupy the young PN region of this diagram, whereas our SySt-3 and the known SySt-1 of IC10 are placed in the region of the evolved PNe. Altogether this seems to indicate that not only two of the (possible and likely) SySts in NGC 205 but also other known SySts are misplaced in this diagram, probably because of the interplay of other effects than the physical conditions of the two kinds of nebulae. Gutierrez-Moreno et al. (1995) also pointed out the fact that very young PNe and D-Type SySts are sometimes impossible to be separated in their diagram. We finally note that though the different metallicities of the spirals (Milky Way and M31) versus the dwarf galaxies of the LG might play a role in the diagram, the use of available data indicates that this effect does not appear to be strong enough to significantly change the location of SySts and PNe in the Gutierrez-Moreno et al. (1995) diagram.

ACKNOWLEDGEMENTS

Authors are very grateful to Joanna Mikolajewska, the referee, for her criticisms to the manuscript that allow us to correct mistakes of the first version and add the important discussions to the paper. We also thank Claudio P. Bastos and Roberto Costa for their

critical reading of the manuscript and a number of fruitful discussions. DRG kindly acknowledges the Instituto de Astrofísica de Canarias (IAC), for their hospitality, where part of this work was done. LM acknowledges financial support from PRIN MIUR 2010-2011, project ‘The Chemical and Dynamical Evolution of the Milky Way and Local Group Galaxies’, prot. 2010LY5N2T. SA is supported by CAPES post-doctoral fellowship ‘Young Talents Attraction’ - Science Without Borders, A035/2013. This work was partially supported by FAPERJ’s grant E-26/111.817/2012 and CAPES’s grant A035/2013.

MAST: some of the data presented in this paper were obtained from the Mikulski Archive for Space Telescopes (MAST). STScI is operated by the Association of Universities for Research in Astronomy, Inc., under NASA contract NAS5-26555. Support for MAST for non-HST data is provided by the NASA Office of Space Science via grant NNX13AC07G and by other grants and contracts.

HST: based on observations made with the NASA/ESA Hubble Space Telescope, and obtained from the Hubble Legacy Archive, which is a collaboration between the Space Telescope Science Institute (STScI/NASA), the Space Telescope European Coordinating Facility (ST-ECF/ESA) and the Canadian Astronomy Data Centre (CADAC/NRC/CSA).

SPITZER: this work is based in part on observations made with the Spitzer Space Telescope, which is operated by the Jet Propulsion Laboratory, California Institute of Technology under a contract with NASA.

REFERENCES

- Allen D. A., 1980, *Astrophys. Lett.*, 20, 131
 Belczyński K., Mikolajewska J., Munari U., Ivison R. J., Friedjung X. M., 2000, *A&AS*, 146, 407
 Ciardullo R., Jacoby G. H., Ford H., Neill J. D., 1989, *ApJ*, 339, 53
 Corradi R. L. M., Magrini L., 2006, in Stanghellini L., Walsh J. R., Douglas N. G., eds, *Proc. ESO Workshop, Planetary Nebulae Beyond the Milky Way*. Springer, Berlin, p. 36
 Corradi R. L. M. et al., 2005, *A&A*, 431, 555
 Ford H. C., Jenner D. C., Epps H. W., 1973, *ApJ*, 183, L73
 Gonçalves D. R., Magrini L., Munari U., Corradi R. L. M., Costa R. D. D., 2008, *MNRAS*, 391, L84
 Gonçalves D. R., Magrini L., Martins L. P., Teodorescu A. M., Quireza C., 2012, *MNRAS*, 419, 854
 Gonçalves D. R., Magrini L., Teodorescu A. M., Carneiro C. M., 2014, *MNRAS*, 444, 1705 (G14)
 Gutierrez-Moreno A., Moreno H., 1996, *PASP*, 108, 972
 Gutierrez-Moreno A., Moreno H., Cortés G., 1995, *PASP*, 107, 462
 Hauschildt P. H., Allard F., Baron E., Schweitzer A., 1999, *ApJ*, 312, 377
 Kaler J. B., Jacoby G. H., 1989, *ApJ*, 345, 871
 Kenyon S. J., Fernández-Castro T., 1987, *AJ*, 93, 938
 Kirkpatrick J. D., Henry T. J., McCarthy D. W., Jr, 1991, *ApJS*, 77, 419
 Kniazev A. Y. et al., 2009, *MNRAS*, 395, 1121
 Leedjävär L., Burmeister M., Mikolajewski M., Puss A., Annuk K., Gañan C., 2004, *A&A*, 415, 273
 Lee H.-W., Heo J.-E., Lee B.-C., 2014, *MNRAS*, 442, 1956
 McConnachie A. W., 2012, *AJ*, 144, 4
 Magrini L., Corradi R. L. M., Munari U., 2003, in Corradi R. L. M., Mikolajewska R., Mahoney T. J. eds, *ASP Conf. Ser. Vol. 303, Symbiotic Stars Probing Stellar Evolution*. Astron. Soc. Pac., San Francisco, p. 539
 Massey P., Gronwall C., 1990, *ApJ*, 358, 344
 Massey P., Strobel K., Barnes J. V., Anderson E., 1988, *ApJ*, 328, 315
 Merrett H. R. et al., 2006, *MNRAS*, 369, 120
 Mikolajewska J., Acker A., Stenholm B., 1997, *A&A*, 327, 191
 Mikolajewska J., Caldwell N., Shara M. M., 2014, *MNRAS*, 444, 586
 Miszalski B., Mikolajewska J., 2014, *MNRAS*, 440, 1410
 Morgan D. H., 1992, *MNRAS*, 258, 639

Munari U., Zwitter T., 2002, *A&A*, 383, 188
Osterbrock D. E., Ferland G. J., 2006, *Astrophysics of Gaseous Nebulae and Active Galactic Nuclei*, 2nd edn. University Science Books, Sausalito, CA
Pereira C. B., Miranda L. F., 2005, *A&A*, 433, 579
Richer M. G., McCall M. L., 1995, *ApJ*, 445, 642
Richer M. G., McCall M. L., 2008, *ApJ*, 684, 1190
Rodríguez-Flores E. R., Corradi R. L. M., Mampaso A., García-Alvarez D., Munari U., Greimel R., Rubio-Díez M. M., Santander-García M., 2014, *A&A*, 567, A49

Schlafly E. F., Finkbeiner D. P., 2011, *ApJ*, 737, 103
Schmid H. M., 1989, *A&A*, 211, L31
Schmid H. M. et al., 1999, *A&A*, 348, 950
Tomova M. T., Tomov N. A., 1999, *A&A*, 347, 151

This paper has been typeset from a \TeX/L\TeX file prepared by the author.